Mine Water and the Environment (2024) 43:104–116
https://doi.org/10.1007/s10230-024-00972-8

TECHNICAL ARTICLE

Tracer Test Method to Confirm Hydraulic Connectivity Between Goafs in a Coal Mine

Qiang Xu[1,2] · Qiangling Yao[1,2] · Furong Wang[1,2] · Lei Xiao[2,3] · Junqiang Ma[1,2] · Fanlong Kong[2,3] · Xiaobei Shang[1,2]

Received: 11 April 2023 / Accepted: 10 February 2024 / Published online: 9 March 2024

Abstract

Improving utilization of mine water in underground reservoirs requires determining the hydraulic connectivity between goafs. In this study, a new method for detecting the hydraulic connectivity between adjacent goafs based on a chemical tracer was proposed. First, based on the geological and mining conditions of the mine, a FLAC^{3D} numerical model was established to analyze the distribution pattern of plastic zones on both sides of the coal pillar after mining, and the range of hydraulic connectivity testing in the goaf was preliminarily determined. Also, a tracer mass calculation model considering the water storage coefficient of goafs was established. The change rates of tracer concentration and water level of the goaf were used as the evaluation indexes for the hydraulic connectivity. The new detection method was applied to abandoned goafs in a coal mine and a plan was proposed to construct a coal mine underground reservoir, using the 31,301–31,307 goaf where the main reservoirs were constructed in the 31,303 and 31,305 goafs while the 31,307 goaf served as the auxiliary one. The 31,301 goaf cannot be utilized from the perspectives of cost and safety.

Keywords Mine water · Chemical tracer method · Coal pillar · Underground reservoir · Water storage coefficient

Introduction

With the depletion of coal resources in eastern mining areas of China, coal mining activities are rapidly shifting to the northwest mining areas that are ecologically fragile. This area, where the average evaporation of surface water is four times as high as the annual precipitation, is characterized by typical arid and semi-arid climate. The proven reserves of coal resources there account for over 70% of the country's total amount but the water resources only account for 9% (National Bureau of Statistics 2020). At the same time, large-scale and high-intensity underground coal mining compromises the integrity of roof rock structure in these areas. The seepage of water from the bedrock aquifer and the Quaternary aquifer into the goaf causes a decrease in the groundwater level, which aggravates deterioration of the ecological environment (Li 2018a). Therefore, clean water resources with reliable sources and stable quality are needed for the coordinated development of coal mining and environmental protection.

Abundant mine water is generated from coal mining activities. The mine water typically has high concentrations of suspended solids due to the existence of impurities such as coal debris and dust. It also contains a certain amount of potentially toxic elements, organic matter, and microorganisms. Consequently, its average utilization rate is only 35% (Gu 2015). The establishment of underground reservoirs in the large underground goaf can effectively help treat the mine water, which provides a new way to address the problem of water shortage in ecologically fragile mining areas (Fan et al. 2020; Song et al. 2020; Wang et al. 2018) (Fig. 1). The underground reservoirs in mines are generally constructed using several adjacent goafs, which jointly perform preliminary purification of mine water through physical sedimentation and partial chemical reactions (Wang et al. 2018; Yao et al. 2020; Zhu et al. 2023). It should be noted that the mine water, after preliminary purification,

✉ Qiangling Yao
yaoqiangling@cumt.edu.cn

1 Key Laboratory of Deep Coal Resource Mining, Ministry of Education, China University of Mining and Technology, Xuzhou 221116, China

2 School of Mines, China University of Mining and Technology, Xuzhou 221116, China

3 GD Construction and Investment Inner Mongolia Energy Co., Ltd, Erdos 017209, China

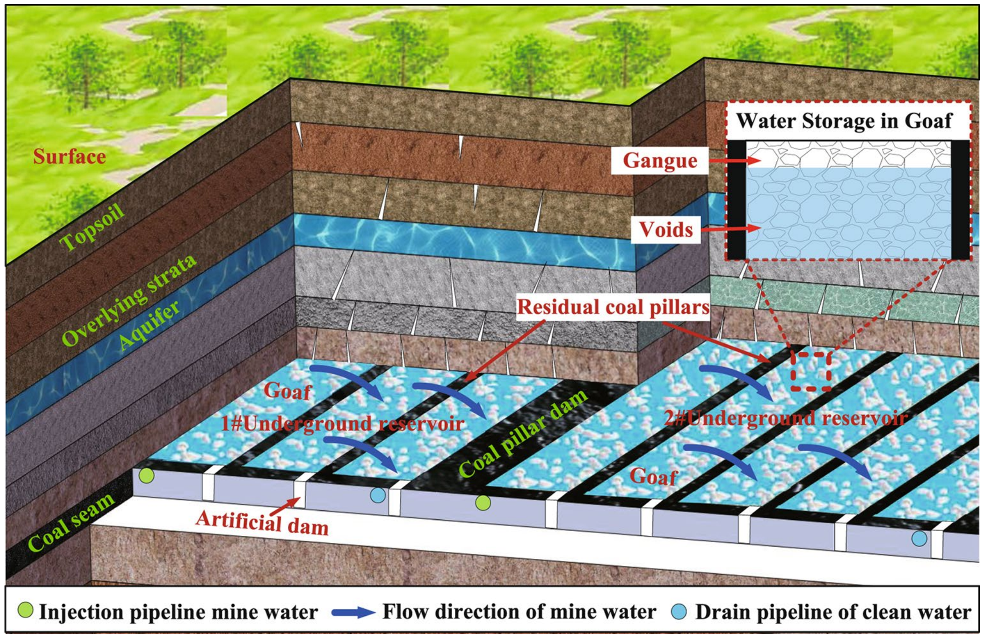

Fig. 1 Schematic diagram of an underground reservoir in a coal mine

still requires further treatment to meet the standards for use. However, the remaining coal pillars between adjacent goafs, which affect the hydraulic connectivity between goafs, weaken the purification effect of goaf gangue on mine water (Qiao et al. 2018; Zhao et al. 2019). Therefore, determining the hydraulic connectivity between goafs on both sides of the remaining coal pillars is crucial for the evaluation of mine water purification capacity of underground reservoirs.

It is assumed that groundwater in different aquifers flows linearly, and two hydraulically connected aquifers share the same hydrochemical properties. On this basis, the hydrochemical method plays an important role in detecting the hydraulic connectivity between groundwater circulation systems and between surface water and groundwater. Based on massive geothermal hydrochemical data, Lin et al. (2007) analyzed the hydraulic connectivity between adjacent geothermal wells and determined the source of a geothermal water supply. Wu et al. (2014, 2015) revealed water flow channels between different confined aquifers by analyzing the distribution of fluoride in two confined aquifers in the mining area. Li et al. (2018b) explored the hydraulic connectivity between confined aquifers and lower coal-bearing aquifers by collecting and analyzing a large number of groundwater samples from mining areas. Li et al. (2016a, b) estimated the hydraulic connectivity between surface water and shallow groundwater using the hydrochemical method, providing reference for the utilization of water resources in arid areas. Through a case study, Oyarzun et al. (2014) demonstrated the applicability and effectiveness of the hydrochemical method for evaluating the interaction between surface water and shallow groundwater.

Tracer testing is a well-developed technique in hydrogeology to study water flow paths, transport processes, and water-rock interactions (Benischke 2021; Dogancic et al. 2020; Fuentes-Lopez et al. 2022; Hazen et al. 2002; Kurukulasuriya et al. 2022; Maqsoud et al. 2012; Muyiwa et al. 2022; Pauwels et al. 2010; Pu et al. 2016; Schladow et al. 2008; Yi et al. 2018). Yin et al. (2014) identified the hydraulic connectivity between shallow and deep groundwater and the water outlets of mine tunnels with tracers such as NaCl and $CaCl_2$, thereby determining the mine water filling conditions. In addition to inorganic salt tracers, isotope tracers are also popular. Researchers have revealed regional hydrogeological characteristics and the interaction between surface water and groundwater using δD, $\delta^{18}O$, $\delta^{34}S$, and $^{87}Sr/^{86}Sr$ as tracers for experiments, providing a scientific basis for comprehensive management of regional surface water and groundwater (Dogancic et al. 2020; Guo et al. 2019; He et al. 2022a; Huang et al. 2018; Jiang et al. 2020; Liu et al. 2021; Zhang et al. 2022). In recent years, the combined use of multiple testing methods has become a research focus. Su et al. (2022) determined the sources of recharge for surface reservoirs by comprehensively adopting methods such as comparative analysis, trend analysis, Pearson correlation analysis, stable isotope analysis, and Morlet wavelet analysis. He et al. (2022) investigated groundwater quality and its influencing factors by combining multiple hydrochemical indicators and dual NO_3^- isotopes ($\delta^{15}N$-NO_3 and $\delta^{18}O$-NO_3). Ma et al. (2016) evaluated the hydraulic connectivity of multiple aquifers in coal mines based on nonlinear principal component analysis and GIS. Frisbee et al. (2022) traced the source of salinity in large agricultural basins by various isotopes and geochemical tracers, providing a basis for changing soil properties through underground drainage.

A mine in the Xinjie mining area discharges underground water at 5,400 m^3/d, and the associated 10,000-m^3 ground reservoir fails to support the treatment of discharged mine water due to its limited storage. Therefore, the mine plans to establish the hydraulic connectivity between abandoned goafs for the purpose of mine water purification, storage, and utilization. In view of the advantages of tracer technology in detecting groundwater flow paths, we proposed a new detection method using a chemical tracer. Subsequently, the proposed method was used to determine the hydraulic connectivity between abandoned goafs. A tracer calculation model was established that considered the water storage coefficient of goafs, and the tracer detection range was estimated by numerical calculation, which is widely used in the field of mining. Hence, the testing efficiency and accuracy of tracer tests were improved. A mine water purification and storage scheme, based on estimation results for this area, was formulated to meet the mine water demands of production, living, and surface ecological restoration in the mining area.

Methods

Basic Principles

Chemical tracing is typically used for researching underground water flow pathways and their correlation with other physicochemical parameters (Benischke 2021). The water flow path can be easily determined by monitoring changes in tracer ion concentrations. Based on the chemical tracer method, a new method for evaluating the hydraulic connectivity between goafs of underground coal mines was proposed. The specific procedure is as follows: after certain amount of an appropriate chemical tracer is injected into the underground reservoir at a water injection station, water samples are collected. The hydraulic connectivity of mine water between goafs is determined by the changes in tracer ion concentrations and water levels.

The basic principles of the new detection method are as follows:

(1) Before the application of the tracer method, the background value is determined by detecting the concentrations of tracer ions in the mine water of the underground reservoir;
(2) A certain amount of appropriate chemical tracer is injected into the underground reservoir at the high-terrain water injection station. Afterwards, water samples are collected at the low-terrain water drainage station. The hydraulic connectivity between goafs of the underground reservoir is determined by the changes in tracer particle concentration in the water samples;
(3) The changes in water levels of different water drainage stations can be used as an auxiliary method to determine the hydraulic connectivity between different goafs of the underground reservoir.

Using water level changes to determine hydraulic connectivity in the enclosed space appears to be the simplest and most convenient method. Based on the geological conditions of the working face, it can be observed that the goaf areas exhibit uneven topography along the strike direction. In such specific geological conditions, relying solely on water level changes to identify the source of mine water is unreliable, while in the tracer method the tracer ion concentration is unique and credible. Therefore, the changes in water levels of different water drainage stations can be used as an auxiliary method to determine the hydraulic connectivity between different goafs of the underground reservoir.

Tracer Mass Estimation

Determining the appropriate chemical tracer type and the necessary tracer mass is the key to the success of a tracer test (Field 2003). The tracer should be selected in line with the following principles: (1) it should be non-toxic, environmentally friendly, cost-effective, and highly available; (2) it should be easily soluble in water, and can move synchronously with mine water without changing the density of groundwater at low concentration; (3) it is unlikely to be absorbed by the gangue; (4) its background value in mine water remains low and barely fluctuates; (5) conservative tracers that boast stable properties are unlikely to trigger chemical reactions with other solutes and geotechnical media in groundwater, and can hardly decompose or deteriorate.

The amount of released tracer mainly depends on the underground reservoir storage capacity, which can be affected by a variety of parameters, including the size of the working face, the mining method, the lithology of coal seam roof and floor, etc. (Song et al. 2020). As the main parameter describing the water storage capacity of a coal mine underground reservoir, the water storage coefficient has attracted the attention of many scholars. Gu (2015) believed that the water storage coefficient is a time-dependent variable determined by the void ratio of rock mass. A model to calculate the underground reservoir storage capacity of coal mine must consider the mining conditions and period of each goaf in the underground reservoir:

$$V\left(h,t\right)=\sum_{i=1}^{n}\int_{0}^{h_i\cos\theta}s'_i\left(z\right)R_i\left(z,t\right)dz \tag{2}$$

where $V(h, t)$ is the volume of underground water storage, m^3; n is the number of goafs constituting the underground reservoir; h_i is the water storage level of the i^{th} goaf, m; θ is coal seam dip angle; s'_i (z) is the water storage area of the i^{th} goaf, m^2; $R_i(z, t)$ is the water storage coefficient of the i^{th} goaf. Without considering the fracture zone, Chen (2016) defined the void ratio of the caving zone as the water storage coefficient. Then, the underground reservoir storage capacity is expressed as:

$$V\left(h,t\right)=\sum_{i=1}^{n}\int_{0}^{h_i\cos\theta}\varphi\left(t\right)s'_i\left(z\right)dz \tag{3}$$

where $\varphi(t)$ is the void ratio of the caving zone.

Based on experience with the tracer method, it is necessary to consider the significance coefficient between the test value and background value of water samples when calculating the tracer mass. That is, when the ratio of the concentration of the tracer ion in water samples to the concentration before tracer release exceeds a certain value, that means that the tracer ion in the mine water has changed significantly. Thus, the tracer mass can be calculated according to Eq. (4):

$$Q=A\nu_1\frac{V\left(h,t\right)}{10^6}=A\frac{\nu_2M_s}{nM_a}\frac{\sum_{i=1}^{n}\int_{0}^{h_i\cos\theta}\varphi\left(t\right)s'_i\left(z\right)dz}{10^6} \tag{4}$$

where Q is the tracer mass, kg; A is the significance coefficient; M_s is the molar mass of the chemical tracer, mg/mol; M_a is the molar mass of the effective tracer, mg/mol; n is the mole number of effective tracer substances in each mole tracer; v_1 is the tracer compounds concentration in mine water before tracer release, mg/m^3; and v_2 is the tracer ion concentration in mine water before tracer release, mg/m^3.

In this paper, the coefficient of significance refers to the amplification factor applied to the background value when determining the mass of the tracer. In tracer experiments, good hydraulic connectivity between the locations of tracer injection and sampling collection is generally assumed when the tracer ion concentration in the collected water sample exceeds the background value. Unfortunately, there are no established values in the literature regarding the degree to which the detected tracer ion concentration should exceed the background value. It is widely recognized that the ion concentration in mine water naturally decreases due to ion adsorption during the flow process (Zhao et al. 2019). Therefore, when calculating the mass of the tracer, it is necessary to amplify the tracer mass using the coefficient of significance to avoid testing errors or unscientific conclusions caused by the concentration reduction of the tracer ions in the flow process.

Most formulas for calculating tracer mass are proposed based on experience, and no formulas can account for all actual testing conditions. Researchers believe that the tracer ion concentration should exceed the background concentration by at least 10.0 times to ensure the accuracy of the results (Field 2003). For example, in a tracer experiment to detect water filling conditions in a coal mine in Inner Mongolia, China, the effective concentration of tracer ions (NaCl) in the water sample was 15 times the background concentration (Yin et al. 2014). In this study, the proposed testing method was applied for the first time to assess hydraulic connectivity between adjacent goaf areas with a coefficient of significance of 10.0.

To determine the coefficient of significance more scientifically, laboratory percolation experiments were conducted on the gangue of the goaf area, attempting to analyze the attenuation characteristics of tracer ions during mine water flows through the goaf area and to provide a reasonable coefficient of significance. However, there is a great difference in sizes between the gangue used in the lab tests and the actual blockiness of the gangue in the goaf area, and thus the experimental results cannot provide a reference for determining the coefficient of significance in tracer experiments. Based on this study, the next step will be experiments on the ion adsorption capabilities of gangue at different scales, to offer guidance for the widespread application of this approach.

Estimation of the Detection Range

Although coal pillars block the connection between mine waters of adjacent goafs, after being disturbed by mining twice, the plastic failure zones formed on both sides of coal pillars can provide channels for mine water flow within coal pillars (Xia et al. 2021). Variable mining conditions inevitably result in coal pillars with different widths in goafs. Under mining disturbance, narrow coal pillars can easily form a connected plastic failure zone, while wide coal pillars may form an unconnected plastic failure zone on both sides; a stable zone with a certain width exists in the middle of wide coal pillars, unfavorable for mine water flow. A reasonable arrangement of measurement stations can be determined in advance using numerical simulation methods and the application scope of tracer methods can be preliminarily determined as the detection range. FLAC^{3D} numerical calculation is a basic method to obtain the range of the plastic failure zones on both sides of coal pillars under complex conditions in the mining field (Liu et al. 2021). Since the parameters of coal and rock seams in numerical models are mainly determined by indoor experiments and their values are conservative, they are effective in evaluating the hydraulic connectivity between goafs on both sides of narrow coal pillars and have been widely used. However, this method fails to accurately determine the hydraulic connectivity of the stable zone in the middle of wide coal pillars. Despite the addition of a fluid model, the simulation results are not convincing (Yao et al. 2019). Further validation of connectivity by tracer testing is required.

Due to the undulating underground terrain of coal mines, the complex layout of roadways and chambers, and the development of many engineering rock fractures, water drainage stations cannot be arranged in an ideal state in tracing tests. Therefore, it is necessary to estimate the detection range through numerical simulation before tracing tests to minimize the testing range. The coal pillars that have undergone complete plastic failure can be excluded from hydraulic connectivity detection, which can save workload and improve test efficiency. For example, Liu et al. (2021) estimated the detection range by FLAC^{3D} numerical simulation before assessing the range of the fracture zone above the working face by the isotope tracing method. The estimation determines the location of the tracer-adding aquifer, and improves testing efficiency and accuracy. In conclusion, the hydraulic connectivity testing method for adjacent goafs proposed in this study is based on on-site tests within the evaluation range of the numerical model.

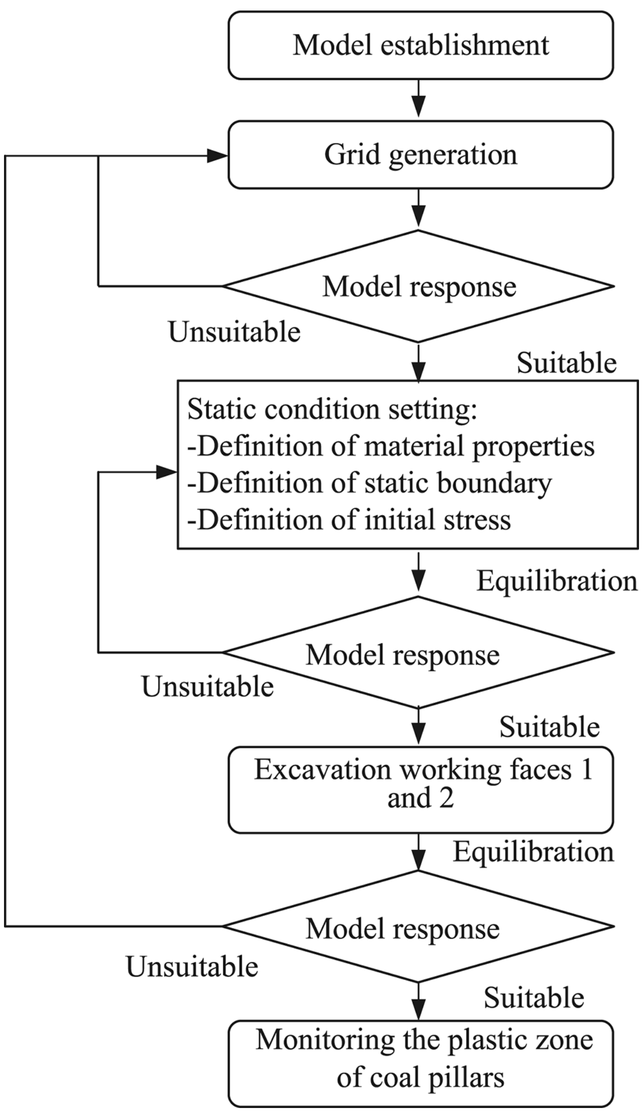

Fig. 2 Numerical simulation procedure

The formation of a plastic failure zone during mining disturbance is a mechanical calculation process. The basic process of analyzing the distribution of plastic failure zones in coal pillars with the FLAC^{3D} numerical model is as follows (Fig. 2):

(1) A numerical model was established based on geological and mining conditions; the coal seam model and parameters were defined; stress and boundary conditions were applied; and calculation continued until the initial stress equilibrium state was reached.
(2) Coal pillars were reserved according to the on-site project design; the working face on both sides of the pillars was excavated; and iterations lasted until a stress equilibrium state was reached.
(3) The range of the plastic failure zone on both sides of the coal pillars was analyzed and the hydraulic connectivity between goafs on both sides of coal pillars was determined.

Injection and Sampling of Tracers

Water injection and drainage are parts of the normal operation of a coal mine underground reservoir, and mine water flows slowly in the reservoir all the time. Considering this, a high-concentration tracer solution was injected via a high-terrain water injection station into the underground reservoir as quickly as possible in a single dose. Driven by pump-induced constant flow, the tracer forms a 'high-concentration slug' in the vicinity of the release point and migrates with the mine water. In this way, the tracer maintains a high concentration that can be easily detected when reaching the water drainage station. It is noteworthy that mine water should be continuously injected at a constant flow rate during the test to ensure water flow in the underground reservoir.

Based on the detection range estimated as detailed above, water samples were strategically collected from different low-terrain water drainage stations to assess the hydraulic connectivity between the various goafs. Each sampling involved all of the water drainage stations, and the sampling frequency was determined according to the scale and water storage capacity of the reservoir. During the test, mine water in the reservoir was discharged at a constant flow rate via all of the water drainage stations, so that the tracer maintained a steady flow state. The collected water samples were immediately sent to the laboratory to determine the tracer ion concentration. Meanwhile, the water level data of each water drainage station in the underground reservoir were obtained to assist the analysis on hydraulic connectivity between different goafs in the underground reservoir.

Determination of Hydraulic Connectivity.

The concentrations of trace ions in water samples from the water drainage stations were compared with their background values. The relative increase of trace ion concentration can be calculated by Eq. (5):

$$\Delta\delta_{Tin} = \frac{\delta_{Tin}}{\delta_{TB}} \tag{5}$$

where $\boldsymbol{\Delta\delta_{Tin}}$ is the relative increase in tracer ion concentration of the n^th^ water sample at the i^th^ water drainage station; $\boldsymbol{\delta_{Tin}}$ is the tracer ion concentration of the n^th^ water sample at the i^th^ water drainage station, mg/m³; and $\boldsymbol{\delta_{TB}}$ is the background value of tracer ion concentration, mg/m^3. The change rate of water level can be calculated by Eq. (6):

$$\Delta Z_i = \frac{Z_{in}}{Z_{iB}} \tag{6}$$

where ΔZ_i is the change rate of water level at the i^{th} water drainage station; Z_{in} is the water level of the n^{th} water sample at the i^{th} water drainage station, m; and Z_{iB} is the background value of water level at the i^{th} water drainage station.

If $\Delta\delta_{Ti}$ is greater than the preset significance coefficient A, the tracer ions have flowed with the mine water to the i^{th} water drainage station, meaning that the i^{th} water drainage station and the water injection station are hydraulically connected. However, if $\Delta\delta_{Ti}$ is smaller than A, the two stations are poorly hydraulically connected. In addition, if ΔZ_i is greater than 1.0 and grows with the amount of test time, the goaf at the i^{th} water drainage station is directly hydraulically connected with the goaf at the i^{th} water drainage station. However, if ΔZ_i is less than 1.0, no direct hydraulic connectivity exists between the two goafs.

Study Area

Location and Geology

The Xinjie mining area is located in the eastern Ordos Plateau, Inner Mongolia Autonomous Region, China. In the hope of realizing the recycling of mine water, a coal mine in this mining area plans to establish an underground reservoir in the abandoned 31,301–31,305 goafs. Since the adjacent goafs have sectional coal pillars of different widths (Fig. 3), it is necessary to test the hydraulic connectivity between goafs in the region to put forward a reasonable construction scheme for the underground reservoir. The mine field covers an area of 196.7 km^2, 12.8 km from north to south and 16.2 km from west to east. The highest elevation is 1,451.8 m and the lowest elevation is 1225.9 m.

The mine field contains 14 minable coal seams, among which the $3-1$ seam is the main mined coal seam. Specifically, the burial depth is 397.1-431.4 m, 430.7 m on average; the thickness is 2.1–7.2 m, 5.3 m on average; the dip angle is 1°-3°. The immediate roof is composed of mudstone and sandy mudstone, about 5.2 m thick, and the main roof is dominated by medium sandstone, about 25.0 m thick. All working faces were recovered by the one-time full-height mining method, and the roof is controlled by the natural caving method. The caving zone used for water storage in the goaf is about 6.8 m high. The void ratio of caving gangue is about 0.2. Affected by mining conditions, the remaining coal pillars between the abandoned 31,301–31,305 goafs are 38 m, 18 m, and 43 m wide, respectively.

Climate and Hydrology

The mine field is a typical accumulation landform where most of the land is covered by aeolian sand. The climate is a semi-arid temperate plateau continental climate, characterized by sparse vegetation, dry air, and rare rain. The annual precipitation is 194.7-531.6 mm, 396.0 mm on average, which is mainly concentrated in July, August and September. The annual evaporation is 2297.4–2833.0 mm, 2534.2 mm on average.

The water system in the mining area is poorly developed and there are no lakes. The northern valleys are distributed in a southwest-northeast direction, with water flowing out of the mining area from south to north. The southern valleys are distributed in a northwest-southeast direction, with water flowing out of the mining area from northwest to southeast. The surface valleys are intermittent rivers. These rivers are mostly dry or have little streams in the dry season, yet they can converge into floods after rainstorm, featuring a large water volume and a short duration.

Mesozoic continental clastic rock is mainly developed in the mining area, followed by Cenozoic semi-cemented and loose rock. The water-bearing rock formations in the mining area fall into three categories: loose porous rock formations, semi-cemented porous rock formations, and fractured-porous clastic rock formations. The surface water in the mining area is undeveloped. Meanwhile, the hydrogeological

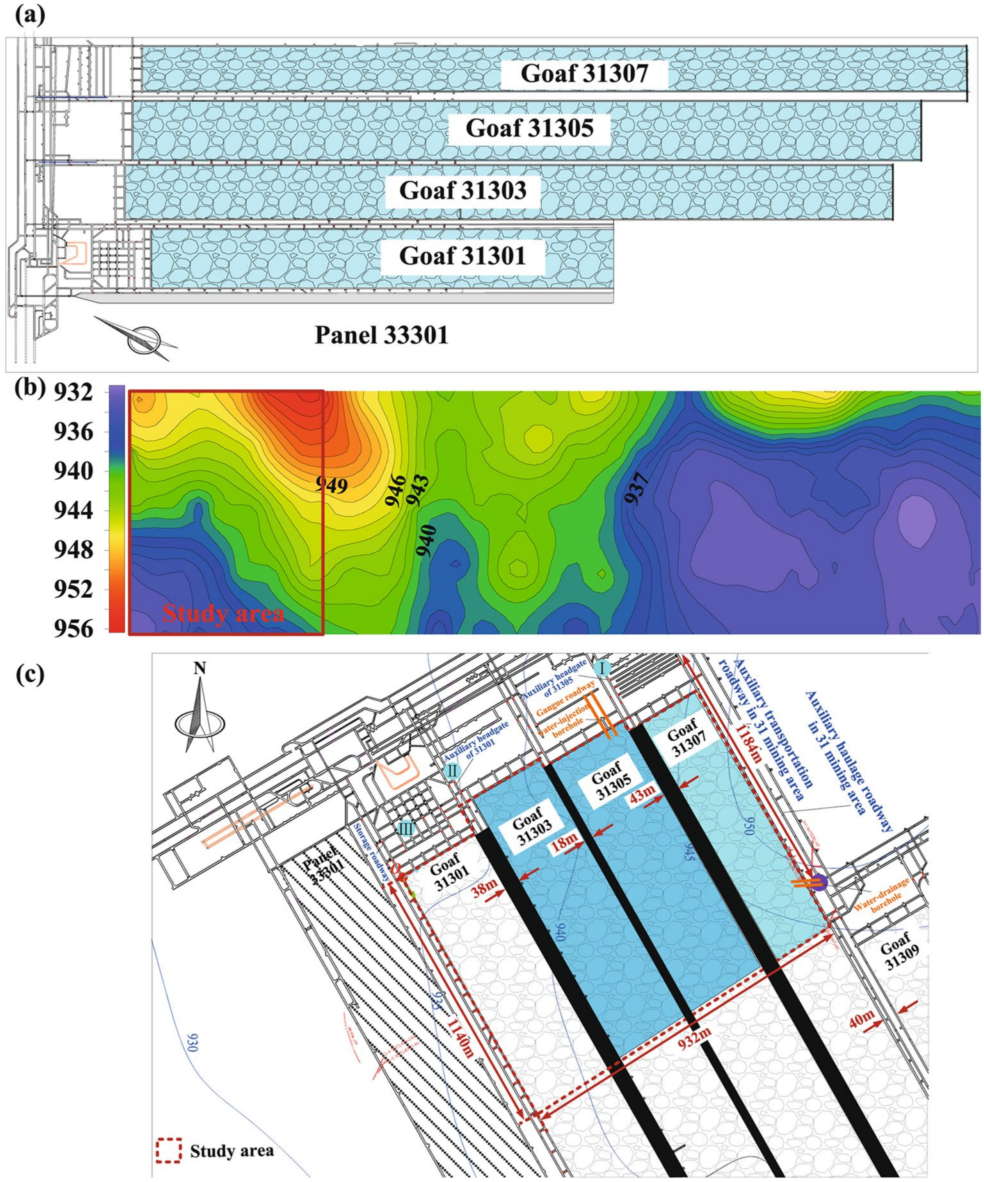

Fig. 3 Plan view of coal face layout : **a** Global map of the goaf, **b** Elevation cloud map of goaf, and **c** Study area map

condition is characterized by underdeveloped fault structures leading to limited hydraulic connectivity, along with the inherently low permeability of the sedimentary rocks in the mining area, which together restrict groundwater flow in the area. The Quaternary loose phreatic aquifers directly receive atmospheric precipitation, while the bedrock aquifers receive atmospheric precipitation and groundwater supply in the shallow area.

Detection Scheme

According to the geological conditions of the test area, three numerical calculation models were established for the three coal pillars that were 18, 38, and 43 m wide, respectively. The working faces on both sides of the coal pillar were 300 m wide. Research revealed that as the working face advanced, the lateral roof behind the working face broke, rotated, and sank synchronously. Consequently, the plastic failure zones on the sides of the coal pillar expanded to the interior and then reached a limit equilibrium position (Yu et al. 2016). The size of the model was defined to be 880 m long, 400 m wide, and 190 m high. When the working face advanced by 100 m, the development characteristics of the plastic failure zones on both sides of the coal pillar were analyzed (Fig. 4a).

The numerical model had a fixed bottom boundary and a free top boundary. The lateral surfaces of the model were fixed to prevent any horizontal displacement, thereby simulating the natural constraints imposed by the surrounding rock masses. The weight of the rock layer above the model was applied to the upper boundary as a uniform load (6 MPa). The Mohr-Coulomb constitutive model was selected as the unit material. Based on the laboratory test results of the coal rock samples, their physical and mechanical parameters were determined according to the Hoek-Brown empirical formula. Furthermore, the mechanical parameters of the coal rock mass were corrected by the trial-and-error method. The mechanical parameters of each rock layer in the numerical model are shown in Table 1. The numerical simulation process is as follows:

(a) In the absence of any excavation activity, the model was calculated to the initial stress equilibrium state.
(b) The mining roadways on both sides of the coal pillar were excavated, and calculation was conducted to the corresponding stress equilibrium state. The simulated range of the plastic zone around the roadway and the field test results of the destressed zone were comparatively analyzed.
(c) Working faces 1 and 2 were sequentially excavated, and calculations were conducted to reach the stress equilibrium state.
(d) Under a changed width of the coal pillar, the above steps were repeated. The distributions of failure zones on both sides of coal pillars with different widths are illustrated in Fig. 4b.

Figure 4b exhibits the distributions of the failure zones that were disturbed by mining activities twice. It can be observed from Fig. 4b that for the 18-m wide coal pillar, the failure zones become connected after the recovery of working faces 1 and 2. The whole coal pillar dam has failed over a large range and lost its bearing capacity. Consequently, the goafs on both sides are connected by failure zones. In contrast, for the 38-m wide coal pillar, the failure zones on both sides are not connected, and an elastic zone of about 7.5 m is retained in the central part. The failure zones on both sides of the 43-m wide coal pillar are not connected, and an elastic zone of about 20.0 m is retained in the central part. However, since the numerical calculation does not consider the expansion of the failure zone under the long-term action of rock weathering, it is necessary to conduct a tracer test on the connectivity between goafs on both sides of the latter two coal pillars.

The three-dimensional elevation map of the 3 – 1 coal seam is depicted based on the relevant wireframe of point elevation data. As presented in Fig. 5, the test area is generally high in the northeast and low in the southwest. The hydraulic connectivity test was conducted in the northwest of the abandoned 31,301–31,307 goafs with a strike length of 1,140 m and a dip length of 932 m. Among them, the highest elevation is 956.5 m and the lowest elevation is 931.7 m, the difference between the two being 24.7 m.

The water injection station was arranged at a position about 1,184 m away from the entry of the auxiliary transportation roadway in the 31 panel. The 1# water drainage station was arranged at a position 69.0 m from the entry of the 31,305 auxiliary transportation roadway. The 2# water drainage station, which was aimed to detect the hydraulic connectivity between goafs on both sides of the 43-m wide coal pillar, was arranged at a position 197.0 m away from the entry of the 31,301 auxiliary transportation roadway. The 3# water drainage station, which was used to detect the hydraulic connectivity between the goafs on both sides of the 38-m wide coal pillar, was arranged in the storage roadway. The specific locations are displayed in Figs. 3 and 5.

Considering the chemical composition of the mine water and the solubility, mobility, and cost of tracers, KI was selected as the tracer for this test. Before the test, water samples were collected and analyzed at the water drainage stations. The background values of iodine ion concentrations at 1#, 2#, and 3# water drainage stations were 39.3, 55.7, and 38.0 mg/m^3, respectively, with an average of 44.3 mg/m^3. To ensure the effectiveness of the tracer test, the significance coefficient (A) in Eq. (4) was determined to be 10 (Liu et al. 2021; Yin et al. 2014). According to Eq. (4), the mass of

Table 1 Mechanical properties of coal rock strata in the model

Coal rock strata	Thickness (m)	Density (kg.m^{-3})	Elastic modulus (GPa)	Poisson's ratio	Cohesion (MPa)	Friction angle (°)	Tensile strength (MPa)
Siltstone	34.0	2,440	3.51	0.17	5.16	34.58	1.50
Fine sandstone	8.0	2,269	1.61	0.17	4.37	31.83	0.51
Siltstone	34.0	2,327	5.86	0.15	5.66	36.00	0.89
Medium sandstone	6.0	2,480	3.45	0.09	4.24	31.34	0.48
Sandy mudstone	26.0	2,222	5.35	0.19	6.26	37.44	1.08
Mudstone	2.0	2,428	6.30	0.19	4.92	33.83	0.67
3 – 1 coal seam	6.0	1,387	0.99	0.21	3.05	26.09	0.61
Mudstone	6.0	2,408	6.75	0.18	5.80	31.77	0.68
Siltstone	26.0	2,350	4.69	0.17	6.46	33.58	0.86
Fine sandstone	16.0	2,154	5.49	0.21	5.10	29.48	0.50
Siltstone	6.0	2,410	6.89	0.24	5.85	31.90	0.69
Fine sandstone	20.0	2,549	5.58	0.19	6.66	34.06	1.50

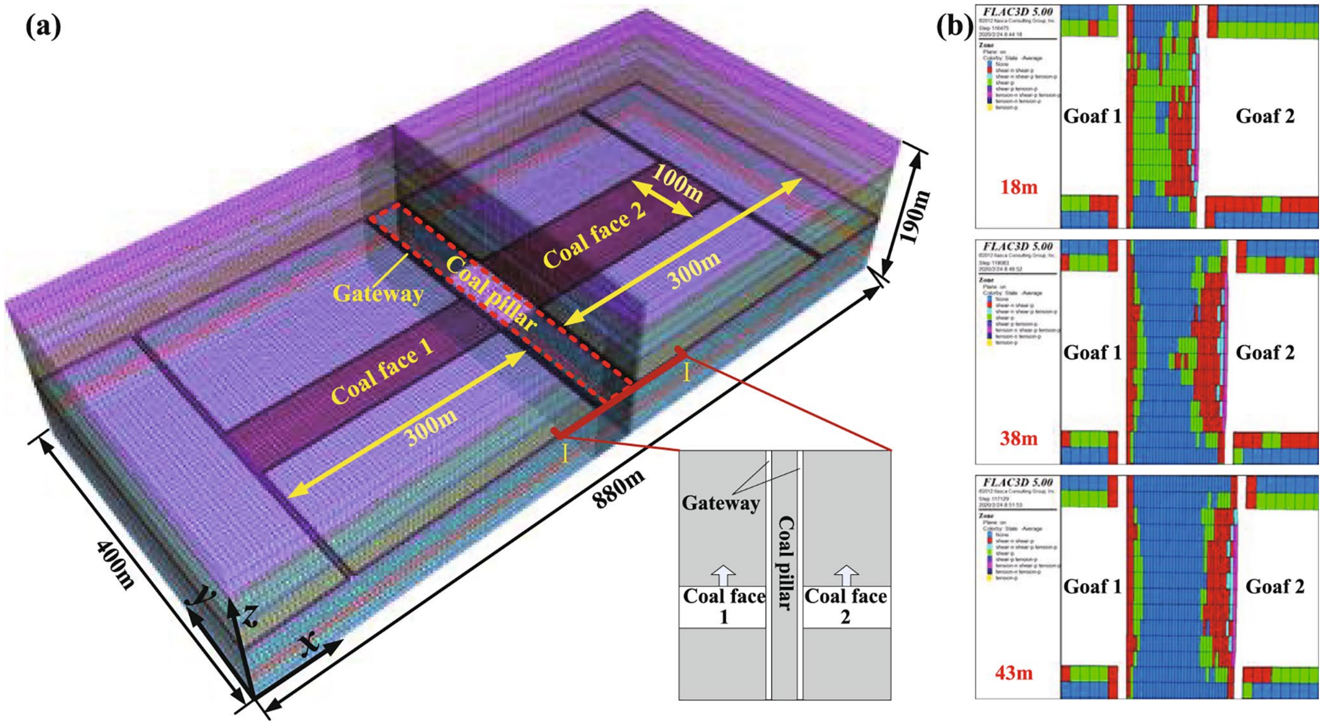

Fig. 4 Goaf connectivity simulation: **a** Configuration of the FLAC^{3D} model, and **b** Distributions of failure zones of coal pillars

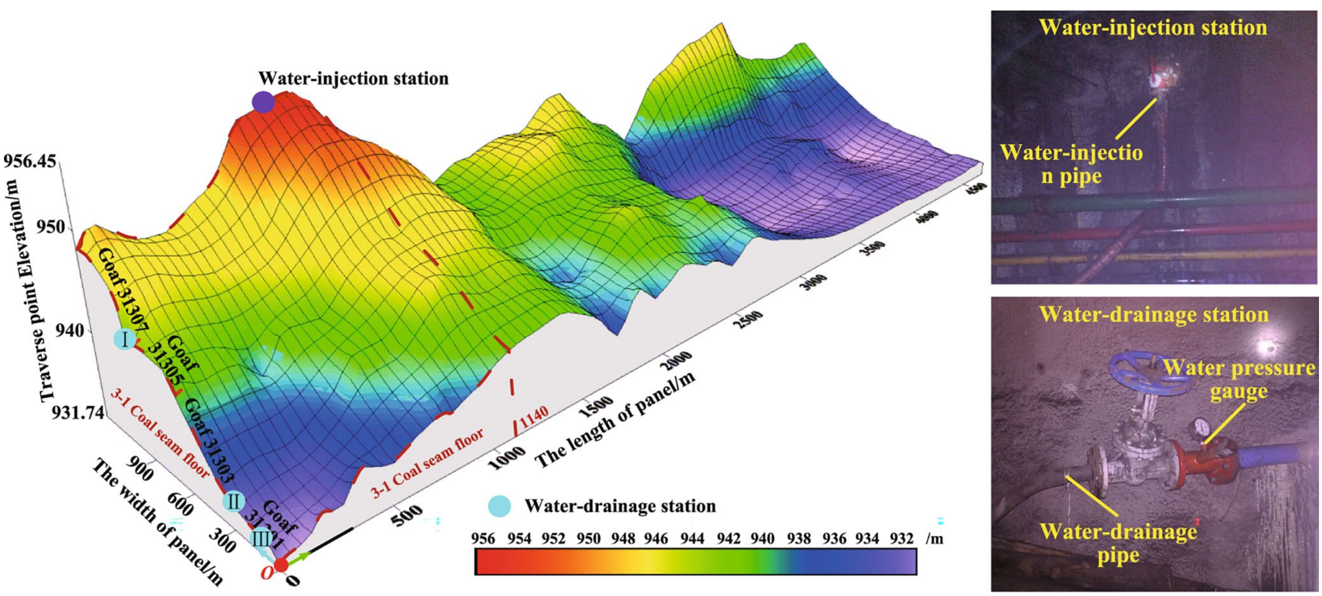

Fig. 5 Three-dimensional elevation map of the 3 – 1 coal seam

potassium iodide tracer was calculated to be 820 kg. Considering the adsorption effect of the goaf gangue, the actual release of potassium iodide tracer was 1,000 kg in this test.

The new measurement method was applied to the abandoned 31,301–31,307 goafs, and one metric ton of potassium iodide was injected into the goaf for tracing. According to the principle of tracer preparation and injection, potassium iodide was dissolved in the coal mine's underground clean water tank in two batches (each with a volume of 12 m^3), for a total volume of 24 m^3. Then, the prepared tracer solution was pumped into the underground reservoir at a flow rate of 50 m^3/h for 4.5 h. During the test, mine water was continuously injected into the underground reservoir from the clean water tank. It should be noted that to ensure the continuity of water injection, the external water delivery pipe will continue to inject mine water into the pool until the tracer experiment is completed.

Considering the scope of the experiment and with reference to the experience of successful cases, water samples were collected at each water drainage station after five days of tracer release. After being labeled with relevant information such as time and location, the water samples were sent to the water quality laboratory. Water samples were collected every two days and the water level at the sampling points were recorded. The variations of iodine ion concentration and water level at each water drainage station are illustrated in Fig. 7.

Result Analysis

It can be seen from Fig. 6 that after the release of the potassium iodide tracer, the trends of I^- concentrations at different water drainage stations differ. For water samples from the 1# water drainage station, the I^- concentration first remains unchanged and then increases notably on the 12th day after the release of the tracer, with the maximum of 615.7 mg/m^3. The change rate of I^- concentration is about 15.0, greater than the significance coefficient 10.0, which suggests that the water injection position is hydraulically connected with the water drainage position. Since the 1# water drainage station and the water injection station are located in the same goaf, we did not continue to monitor the water sample and water level of the 1# water drainage station. In contrast, for the samples from the 2# and 3# water drainage stations, within 129 days of tracer test, the I^- concentration does not present significant changes, with maxima of 67.1 mg/m^3 and 54.5 mg/m^3, respectively. The concentration change rates are about 1.2 and 1.1, much less than the significance coefficient 10.0. It is concluded that the I^- concentrations of the 2# and 3# water drainage stations fluctuate around the background value during the test, which is indicative of poor or no direct hydraulic connectivity between goafs on both sides of the 43 and 38 m wide coal pillars.

A goaf is a relatively enclosed space, and the variation of its internal water level is always important for monitoring mine safety. Accumulated water in goafs generally comes from roof water. Engineering practice found that the water level in the goafs hardly rises in a short time unless there is massive external water supply. Therefore, during tracing tests, it is helpful to monitor water level variations in adjacent goafs to determine the hydraulic connectivity between them. The water volume variations of the underground reservoir and water level of the 2# and 3# water drainage stations are shown in Fig. 7. As exhibited in Fig. 7, the water injection volume exceeds the water-drainage volume in the test area throughout the test. However, the water level change rates of the 2# and 3# water drainage stations are less than 1, and decrease with the increase of test times, that is, the water level continuously falls. Especially for the 3# water drainage station, after the 85th day of the test, the water level is reduced to 0, which further verifies that the goafs on both sides of the 43 and 38 m wide coal pillars are not directly hydraulically connected.

Based on the hydraulic connectivity test results and the production and geological conditions, underground reservoirs were established in the 31,303–31,307 goafs where the main reservoir were constructed in the 31,303 and 31,305 goafs while the 31,307 goaf served as the auxiliary one. The classification, purification, storage, and utilization of mine water in the two underground reservoirs were realized with the aid of the 43-m wide coal pillar between goafs. Considering no direct connectivity between the goafs on both sides of the 38-m wide coal pillar and the short distance between the 31,301 goaf and the 33,301 working face, the 31,301 goaf cannot be utilized from the perspective of cost and safety.

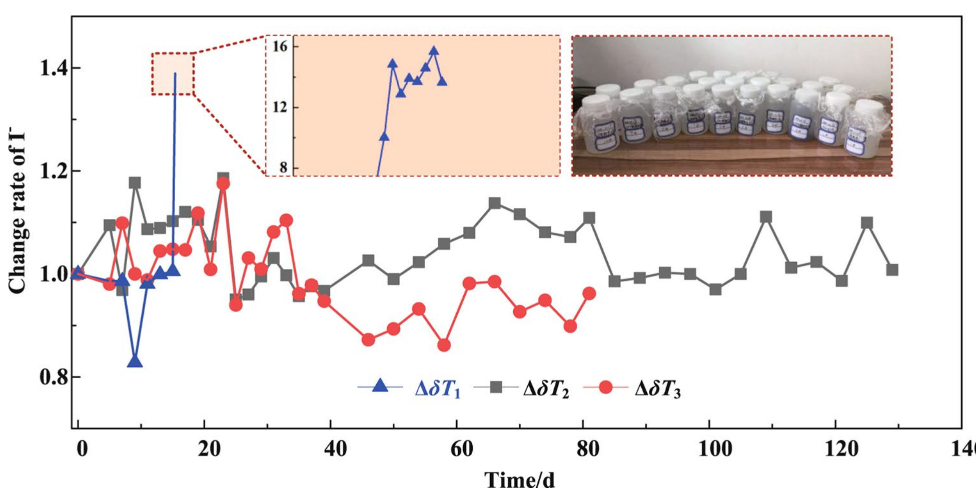

Fig. 6 Tracer test results: **a** Injection of tracer, and **b** Sampling of tracer

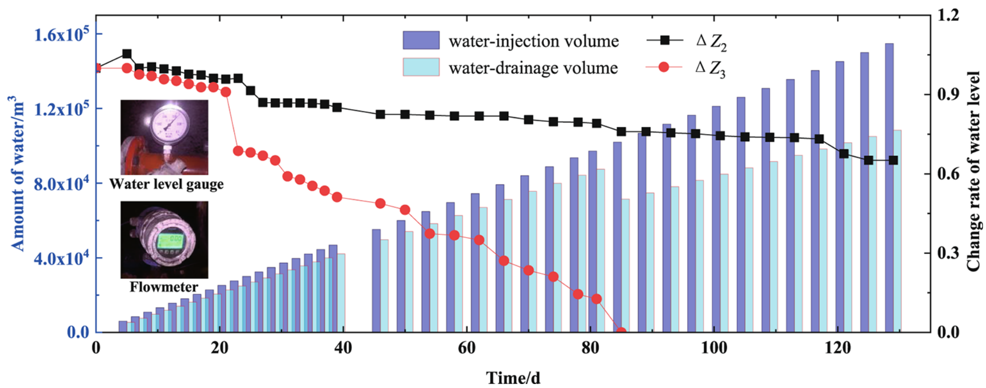

Fig. 7 Variations of water volume and water level with test time

Conclusions

This paper aims to provide a convenient, direct, and accurate method for detecting the hydraulic connectivity between adjacent goafs for field application. The specific procedure of this method is as follows: First, FLAC^{3D} software was used to determine the test range. Afterwards, the chemical tracer mass was determined through the calculation formula considering the water storage coefficient of the goaf and then it was injected into the underground reservoir at the high-terrain water injection station. Finally, the hydraulic connectivity between goafs on both sides of the remaining coal pillar in the underground reservoir was determined by comparing the changes in tracer ion concentration of drainage water and water level at each water drainage station.

The test results demonstrate that the maximum value of the I^- concentration in the water samples at the 1# water drainage station is 615.7 mg/m^3 and the change rate is about 15. In contrast, those in the water samples at the 2# and 3# water drainage stations were 67.1 mg/m^3 and 54.5 mg/m^3 without significant changes, and the change rates were about 1.2 and 1.1, respectively. Such results are indicative of poor or no direct hydraulic connectivity between goafs on both sides of the 43 and 38 m wide coal pillars. Based on the test results, we proposed to use goafs to classify and store mine water for the purpose of meeting water demands for production, living, and surface ecological restoration in the mining area.

The stable chemical tracer method is superior to the physical reverse detection method for its simple data acquisition, high detection accuracy, easy construction and operation, small workload, and low comprehensive cost (Field 2002). Furthermore, this method is free from the interference of working face recovery and underground equipment operation, thus showing strong engineering adaptability. All of these factors should favor its future popularization and application. It should be noted though that this new method fails to give effective and accurate results under complex mining geological conditions, such as close multi-seam mining and fault development. Besides, the test results of this method represent the macroscopic hydraulic connectivity between adjacent goafs in the underground reservoir instead of the microscopic seepage state in coal pillars at any time. In future work, we will further optimize the construction technology and process flow of this method to improve the efficiency of water sample collection and detection rate.

Acknowledgements This work was supported by the Natural Science Foundation of Jiangsu Provincial Basic Research Program (grant BK20220024).

References

Benischke R (2021) Review: advances in the methodology and application of tracing in karst aquifers. Hydrogeol J 29:67–88. https://doi.org/10.1007/s10040-020-02278-9

Chen SS (2016) Research on the key technology of water resources recycling utilization in the underground goaf reservoir in Shendong Mining Area. Dis, Xi'an Univ of science and Technology [in Chinese]

Dogancic D, Afrasiabian A, Kranjcic N, Durin B (2020) Using stable isotope analysis (delta D and delta O-18) and tracing tests to characterize the regional hydrogeological characteristics of Kazeroon County, Iran. Water 12(9):2487. https://doi.org/10.3390/w12092487

Fan JY, Xie HP, Jie C, Jiang DY, Li CB, Tiedeu WN, Ambre J (2020) Preliminary feasibility analysis of a hybrid pumped-hydro energy storage system using abandoned coal mine goafs. Appl Energy 258:114007. https://doi.org/10.1016/j.apenergy.2019.114007

Field MS (2002) Efficient hydrologic tracer-test design for tracer-mass estimation and sample-collection frequency, 1. Method development. Environ Geol 42(7):827–838. https://doi.org/10.1007/s00254-002-0591-2

Field MS (2003) A review of some tracer-test design equations for tracer-mass estimation and sample-collection frequency. Environ Geol 43(8):867–881. https://doi.org/10.1007/s00254-002-0708-7

Frisbee MD, Caffee MW, Camberato JJ, Michalski G (2022) Using multiple isotopic and geochemical tracers to disentangle the sources of baseflow and salinity in the headwaters of a large agricultural watershed. J Hydrol 609:127769. https://doi.org/10.1016/j.jhydrol.2022.127769

Fuentes-Lopez JM, Olias M, Leon R, Basallote MD, Macias F, Moreno-Gonzalez R, Canovas CR (2022) Stream-pit lake interactions in an abandoned mining area affected by acid drainage (Iberian Pyrite belt). Sci Total Environ 833:155224. https://doi.org/10.1016/j.scitotenv.2022.155224

Gu DZ (2015) Theory framework and technological system of coal mine underground reservoir. J China Coal Soc 40(2):239–246. https://doi.org/10.13225/j.cnki.jccs.2014.1661
Guo QL, Yang YS, Han YY, Li JL, Wang XY (2019) Assessment of surface–groundwater interactions using hydrochemical and isotopic techniques in a coalmine watershed, NW China. Environ Earth Sci 78(3):91. https://doi.org/10.1007/s12665-019-8053-2
Hazen JM, Williams MW, Stover B, Wireman M (2002) Characterisation of acid mine drainage using a combination of hydrometric, chemical and isotopic analyses, Mary Murphy Mine, Colorado. Environ Geochem Health 24(1):1–22. https://doi.org/10.1023/A:1013956700322
He S, Li PY, Su FM, Wang D, Ren XF (2022) Identification and apportionment of shallow groundwater nitrate pollution in Weining Plain, northwest China, using hydrochemical indices, nitrate stable isotopes, and the new bayesian stable isotope mixing model (MixSIAR). Environ Pollut 298:118852. https://doi.org/10.1016/j.envpol.2022.118852
He XD, Li PY, Shi H, Xiao YX, Guo YA, Zhao HH (2022) Identifying strontium sources of flowback fluid and groundwater pollution using Sr-87/Sr-86 and geochemical model in Sulige Gasfield. China Chemosphere 306:135594. https://doi.org/10.1016/j.chemosphere.2022.135594
Huang XJ, Wang GC, Liang XY, Cui LF, Ma L, Xu QY (2018) Hydrochemical and stable isotope (delta D and delta O-18) characteristics of groundwater and hydrogeochemical processes in the Ningtiaota Coalfield, northwest China. Mine Water Environ 37(1):119–136. https://doi.org/10.1007/s10230-017-0477-x
Jiang CF, Gao XB, Hou BJ, Zhang ST, Zhang JY, Li CC, Wang WZ (2020) Occurrence and environmental impact of coal mine goaf water in karst areas in China. J Clean Prod 275:123813. https://doi.org/10.1016/j.jclepro.2020.123813
Kurukulasuriya D, Howcroft W, Moon E, Meredith K, Timms W (2022) Selecting environmental water tracers to understand groundwater around mines: opportunities and limitations. Mine Water Environ 41(2):357–369. https://doi.org/10.1007/s10230-022-00845-y
Li PY (2018a) Mine Water problems and solutions in China. Mine Water Environ 37(2):217–221. https://doi.org/10.1007/s10230-018-0543-z
Li PY, Wu JH, Qian H (2016a) Preliminary assessment of hydraulic connectivity between river water and shallow groundwater and estimation of their transfer rate during dry season in the Shidi River, China. Environ Earth Sci 75(2):99. https://doi.org/10.1007/s12665-015-4949-7
Li PY, Zhang YT, Yang NA, Jing LJ, Yu PY (2016b) Major ion chemistry and quality assessment of groundwater in and around a mountainous tourist town of China. Expos Health 8(2):239–252. https://doi.org/10.1007/s12403-016-0198-6
Li PY, Wu JH, Tian R, He S, He XD, Xue CY, Zhang K (2018b) Geochemistry, hydraulic connectivity and Quality Appraisal of Multilayered Groundwater in the Hongdunzi Coal Mine, Northwest China. Mine Water Environ 37(2):222–237. https://doi.org/10.1007/s10040-014-1170-9
Lin XY, Taboure A, Wang XY, Liao ZS (2007) Use of a hydrogeochemical approach in determining hydraulic connection between porous heat reservoirs in Kaifeng area, Henan, China. Appl Geochem 22(2):276–288. https://doi.org/10.1016/j.apgeochem.2006.11.006
Liu XS, Fan DY, Tan YL, Ning JG, Song SL, Wang HL, Li XB (2021) New detecting method on the connecting fractured zone above the coal face and a case study. Rock Mech Rock Eng 54(8):4379–4391. https://doi.org/10.1007/s00603-021-02487-y
Ma L, Qian JZ, Zhao WD, Curtis Z, Zhang RG (2016) Hydrogeochemical analysis of multiple aquifers in a coal mine based on nonlinear PCA and GIS. Environ Earth Sci 75(8):716. https://doi.org/10.1007/s12665-016-5532-6
Maqsoud A, Bussiere B, Aubertin M, Plante B, Cyr J (2012) Tracer tests to evaluate hydraulic residence time in limestone drains: case study of the Lorraine site, latulipe, Quebec, Canada. Int J Min Reclam Env 26(4):275–291. https://doi.org/10.1080/17480930.2011.613567
Muyiwa MO, Mojisola RU, Kayode JO, Charity AO, Taiye BA, Mohammad V, Mark T (2022) Environmental risks assessment of kaolin mines and their brick products using Monte Carlo simulations. Earth Syst Environ 6:157–174. https://doi.org/10.1007/s41748-021-00266-x
National Bureau of Statistics (2020) China Statistical Yearbook-2020. China Statistics, Beijing. (in Chinese)
Oyarzun R, Barrera F, Salazar P, Maturana H, Oyarzun J, Aguirre E, Alvarez P, Jourde H, Kretschmer N (2014) Multi-method assessment of connectivity between surface water and shallow groundwater: the case of Limari River basin, north-central Chile. Hydrogeol J 22(8):1857–1873. https://doi.org/10.1007/s10040-014-1170-9
Pauwels H, Pettenati M, Greffie C (2010) The combined effect of abandoned mines and agriculture on groundwater chemistry. J Contam Hydrol 115(1–4):64–78. https://doi.org/10.1016/j.jconhyd.2010.04.003
Pu CS, Jing C, He YL, Gu XY, Zhang ZY, Wei JK (2016) Multistage interwell chemical tracing for step-by-step profile control of water channeling and flooding of fractured ultra-low permeability reservoirs. Pet Explor Devel 43(4):679–688. https://doi.org/10.1016/S1876-3804(16)30079-9
Qiao W, Li WP, Li T, Zhang X, Wang YZ, Chen YK (2018) Relevance between hydrochemical and hydrodynamic data in a deep karstified limestone aquifer: a mining area case study. Mine Water Environ 37(2):393–404. https://doi.org/10.1007/s10230-017-0506-9
Schladow SG, Clark JF (2008) Use of tracers to quantify subsurface flow through a mining pit. Ecol Appl 18(8):A55–A71. https://doi.org/10.1890/06-0998.1
Song HQ, Xu JJ, Fang J, Cao ZG, Yang LZ, Li TX (2020) Potential for mine water disposal in coal seam goaf: investigation of storage coefficients in the Shendong mining area. J Clean Prod 244:118646. https://doi.org/10.1016/j.jclepro.2019.118646
Su FM, Li PY, Fida M (2022) Dominant factors influencing changes in the water quantity and quality in the Dianshi Reservoir, east China. Hum Ecol Risk Assess 28(3–4):387–407. https://doi.org/10.1080/10807039.2022.2053355
Wang QQ, Li WP, Li T, Li XQ, Liu SL (2018) Goaf water storage and utilization in arid regions of northwest China: a case study of Shennan coal mine district. J Clean Prod 202:33–44. https://doi.org/10.1016/j.jclepro.2018.08.123
Wu JH, Li PY, Qian H, Duan Z, Zhang XD (2014) Using correlation and multivariate statistical analysis to identify hydrogeochemical processes affecting the major ion chemistry of waters: a case study in Laoheba phosphorite mine in Sichuan, China. Arab J Geosci 7(10):3973–3982. https://doi.org/10.1007/s12517-013-1057-4
Wu JH, Li PY, Qian H (2015) Hydrochemical characterization of drinking groundwater with special reference to fluoride in an arid area of China and the control of aquifer leakage on its concentrations. Environ Earth Sci 73(12):8575–8588. https://doi.org/10.1007/s12665-015-4018-2
Xia Ze,Yao QL, Meng GS, Xu Q, Tang CJ, Zhu L, Wang WN, Shen Q (2021) Numerical study of stability of mining roadways with 6.0-m section coal pillars under influence of repeated mining. Int J Rock Mech Min Sci 138:104641. https://doi.org/10.1016/j.ijrmms.2021.104641
Yao QL, Hao Q, Chen XY, Zhou BJ, Fang J (2019) Design on the width of coal pillar dam in coal mine groundwater reservoir. J China Coal Soc 44(3):891–899. https://doi.org/10.13225/j.cnki.jccs.2018.6012

Yao QL, Xia Z, Tang CJ, Zhu L, Wang WN, Chen T, Tan YM (2020) Characteristics of heavy metal ion adsorption by silty mudstones in coal mine goafs. Geofluids 2020: 8560151, https://doi.org/10.1155/2020/8560151

Yi P, Yang J, Wang YD, Mugwanezal VD, Chen L, Aldahan A (2018) Detecting the leakage source of a reservoir using isotopes. J Environ Radioact 187:106–114. https://doi.org/10.1016/j.jenvrad.2018.01.023

Yin SX, Xu B, Xu H, Xia XX (2014) The application of chemical tracer experiments on exploring the mine water filling conditions. J China Coal Soc 39(1):129–134. https://doi.org/10.13225/j.cnki.jccs.2013.0492

Yu YX, Huang RB, Wang BQ (2016) Analysis on limit equilibrium zone of coal pillar in mining roadway based on mechanical model of elastic foundation beam. J Eng Mech 142(4):04016009. https://doi.org/10.1061/(ASCE)EM.1943-7889.0001032

Zhang L, Li PY, He XD (2022) Interactions between surface water and groundwater in selected tributaries of the Wei River (China) revealed by hydrochemistry and stable isotopes. Hum Ecol Risk Assess 28(1):79–99. https://doi.org/10.1080/10807039.2021.2016054

Zhao L, Sun C, Yan PX, Zhang Q, Wang SD, Luo SH, Mao YX (2019) Dynamic changes of nitrogen and dissolved organic matter during the transport of mine water in a coal mine underground reservoir: column experiments. J Contam Hydrol 223:103473. https://doi.org/10.1016/j.jconhyd.2019.03.005

Zhu L, Yao QL, Xu Q, Li YH, Li XH (2023) Experimental study on the purification mechanism of mine water by coal gangue. Water 15(4):697. https://doi.org/10.3390/w15040697